

Optical detection and phonon bottleneck of the direct decay within the $\bar{E}(^2E)$ state of ruby

J. I. Dijkhuis, K. Huibregtse, and H. W. de Wijn

Fysisch Laboratorium, Rijksuniversiteit, P.O. Box 80.000,

3508 TA Utrecht, The Netherlands

(Received 12 April 1979)

Direct relaxation within the optically excited $\bar{E}(^2E)$ level of 700-ppm ruby is investigated in magnetic fields up to 65 kG making an angle to the c axis. At low pump intensities, the experimental relaxation rates are found to be in excellent agreement with the theory by Blume *et al.*, predicting a fifth-power dependence on field and a $\cos^3\theta \sin^2\theta$ dependence on orientation. The observed proportionality constant of $4.7 \times 10^{-19} \text{ G}^{-5} \text{ s}^{-1}$ is close to the theoretical estimate based on static experiments in ruby. When increasing optical pumping, the phonon-bath conduction is demonstrated to become the limiting process due to resonant trapping of the phonons. Following pulsed excitation, a prolonging of the decay time by a factor up to 13 is attained at excited-state concentrations $N^* \sim 2 \times 10^{17} / \text{cm}^3$. In stationary experiments, a nonlinear increase with N^* is observed of the equilibrium population of the upper Zeeman level of \bar{E} to over a decade above the nonbottlenecked value, corresponding to bottlenecking factors of over ~ 200 . Under the assumption of a constant phonon lifetime of the order of the flight time through the illuminated region, rate equations appear to consistently account for the experiments. A Gaussian-type resonance line, fully homogenized supposedly by magnetic interactions with the surrounding Al nuclei and Cr^{3+} ions, explains the lattice-bath equilibration. Finally, the prospect is discussed of using the \bar{E} direct transition in ruby as a tunable phonon generator and detector with bandwidth 0.002 cm^{-1} in the practical frequency range of $2\text{--}15 \text{ cm}^{-1}$.

I. INTRODUCTION

During the last few years, a series of experiments has led to a renewed interest in the ruby system, in particular with regard to nonequilibrium distributions of 29 cm^{-1} phonons resonant between the optically excited Kramers doublets $\bar{E}(^2E)$ and $2\bar{A}(^2E)$ of Cr^{3+} . At temperatures where thermalization is absent, such a bottlenecking of phonons is reflected in the populations of these levels, which in turn can be sensitively monitored by the intensities of the various components of the R_1 and R_2 fluorescent decays. Besides the detection sensitivity, the ruby system offers versatility in varying the physical conditions that affect the bottlenecking, such as the concentration of resonant centers and the physical size of the region in which they are contained. After initial evidence of bottlenecking of 29 cm^{-1} phonons by Geschwind *et al.*,¹ Renk *et al.*² observed resonant absorption and imprisonment of these phonons, produced by short heat pulses, through the development of the R_2 fluorescence when the phonons pass the optically excited region. Experiments in the stationary case³ revealed a nonlinear behavior of the intensity of the R_2 fluorescent line as a function of the R_1 intensity, which is due to multiple interruption of optically generated 29 cm^{-1} phonons. In addition, the dependence of the bottlenecked R_2 intensity on

magnetic field provided a new technique to probe the spectral width of the bottlenecked phonons, and to investigate their spectral diffusion. Meltzer and Rives⁴ studied the temporal decay of optically generated 29 cm^{-1} phonons following a short light pulse, to find it slowed down upon increasing the concentration of excited Cr^{3+} . They took the phonon lifetime limited by anharmonic decay and spatial propagation. Subsequently, conclusive evidence for spatial diffusion was found in a third-power dependence of the R_2 on R_1 intensities when the excitation zone is reduced in size.⁵ Recently, there has also been extensive theoretical work⁶ on energy transfer in inhomogeneously broadened systems, with special attention to ruby. The important interaction here is the exchange between the Cr^{3+} ions. More specifically, the transfer at low temperatures is believed to be governed by exchange processes involving a resonant phonon transition within 2E . It is finally worth mentioning, although only remotely related to the present study, that the ruby system has been utilized to demonstrate the occurrence of Anderson localization.⁷

In this paper, it is first shown that in a magnetic field at an angle to the c axis, and at low temperatures, the direct process between the Zeeman components of the \bar{E} state may become several orders of magnitude faster than both the Orbach relaxation

within \bar{E} via $2\bar{A}$ and the radiative decay to the ground state. The observed magnetic field dependence and the angular dependence will in fact be found to be in excellent agreement with earlier theoretical predictions by Blume *et al.*⁸ Additionally, it will be demonstrated that the phonon system resonant with the direct transition within \bar{E} can be driven to bottlenecking conditions, both under continuous and pulsed optical pumping. The combination of sensitivity through optical detection, the narrowness of the transition, the flexibility of tuning, and the feasibility of bottlenecking offer unique perspectives for utilizing ruby as a highly monochromatic generator and highly energy-selective detector of phonons in a possibly practical range of 2–15 cm^{-1} .

II. SPIN-LATTICE RELAXATION OF THE \bar{E} STATE

The spin-lattice relaxation between the Zeeman components of the \bar{E} state of ruby is governed by several processes. In this section, a number of *a priori* considerations are given, in view of earlier theoretical and experimental work on this system.

In particular during the sixties, much experimental and theoretical work has been done on the direct spin-lattice relaxation of paramagnetic ions in the ground state.⁹ The occurrence of phonon bottlenecking was a major point of interest, but also raised substantial complications in comparing theoretical spin-lattice relaxation times with experiment. Although the predicted linear temperature dependence of direct spin-lattice relaxation found wide experimental verification, only very few experimental data exist on the magnetic field and angular dependences, clearly due to the resonance character of the experimental methods (EPR), which does not easily allow variation of the field. In a number of cases,^{9–12} theoretical magnetic field and angular dependences have been confirmed by experiment, although not simultaneously in one system. Quantitative comparison of the prefactor could, however, not be achieved, since the constants appearing in the equations are hard to estimate.

As already noted by Kiel in 1961,¹³ the theory of direct spin-lattice relaxation can equally well be applied to excited states. Blume *et al.*⁸ calculated the spin-lattice relaxation rates of various processes within the 2E manifold of ruby. The rates of the spin-flip and the non-spin-flip transitions from $2\bar{A} \rightarrow \bar{E}$ were computed, by use of static strain data on the R fluorescent lines. Their results turned out to differ by less than a factor of four from the observed spontaneous decay times,^{1,14} which are about 15 ns for spin flip and 1 ns for non spin flip. In addition, they considered the direct process within the \bar{E} state, which turned out to be quite different from the $2\bar{A} \rightarrow \bar{E}$ decay processes. The point is that an electric potential cannot couple the states of a Kramers doub-

let unless a magnetic field admixes other states. In case an applied magnetic field has a component perpendicular to the c axis, the direct process may indeed compete with the radiative decay of \bar{E} ($\tau_R = 3.7$ ms). The result of Blume *et al.* for the direct relaxation time T_{1d} within the \bar{E} state of ruby is [Eq. (33) of their paper]

$$1/T_{1d} \propto H^5 \cos^3 \theta \sin^2 \theta \coth(\delta/2kT), \quad (1)$$

where H is the magnetic field, θ the angle of the field to the c axis, and δ the Zeeman splitting of the \bar{E} state. The proportionality factor is evaluated by substituting the appropriate values for the ruby system to be $2.7 \times 10^{-19} \text{ G}^{-5} \text{ s}^{-1}$, yielding a direct relaxation time of $T_{1d} = 1.25$ ms at 1 K for a magnetic field of 26 kG applied at 45° to the c axis.

The optically excited \bar{E} state in ruby is an ideal system to experimentally verify the theoretical predictions on the direct relaxation time. The crux is that both the establishment of non-Boltzmann equilibrium and the monitoring of the relaxing populations can be done by optical methods in contrast to the situation in a fixed-field EPR experiment. Another advantage of ruby is that with optical detection one observes the decays of integrated populations, thereby eliminating effects of diffusion from one inhomogeneous packet to another. Finally, the relevant parameters in the prefactor of Eq. (1) are quite well known. There remain a few complications originating from Orbach relaxation of \bar{E} , with $2\bar{A}$ as intermediary, and phonon bottlenecking. These can, however, be reduced by a suitable choice of the experimental conditions, and their residual effects can be accounted for to extract pure \bar{E} direct relaxation rates.

The Orbach relaxation within the \bar{E} level via $2\bar{A}$, induced by the thermal phonons, has been studied in detail by Geschwind *et al.*¹ in the range 2.8 to 4.2 K. Because of the $\exp(-\Delta/kT)$ dependence ($\Delta = 29 \text{ cm}^{-1}$), the Orbach relaxation time extrapolated to 2 K, below which our experiments were done, is already three orders of magnitude larger than the radiative decay. However, Geschwind *et al.* observed a speedup of the relaxation at 1.5 K with increasing pump light intensity, which was ascribed to nonequilibrium resonant 29 cm^{-1} phonons generated in the fast nonradiative decay $2\bar{A} \rightarrow \bar{E}$ of the optical pumping cycle. By now many experiments have proved strong bottlenecking of these phonons at high excited-state concentrations.^{2–4} With a pulsed light source, as we have used, a nonequilibrium population distribution over the \bar{E} levels is established by excitation selective due to spin memory via the broad bands 4T_1 and 4T_2 .^{15,16} After the pulse the 29 cm^{-1} phonons generated in the $2\bar{A} \rightarrow \bar{E}$ decay return to thermal equilibrium on a time scale small compared to T_{1d} , even under severe bottlenecking conditions of these phonons. Therefore, the decay of the R_1 com-

ponents following excitation is virtually determined by the direct decay within \bar{E} , in parallel to the radiative decay to the ground state.

At this point, we examine the phonon reabsorption processes within \bar{E} in order to see what low excited-state concentrations are required to minimize phonon bottlenecking of the direct process. Since only $\sim 4\%$ of our ruby sample is illuminated and therefore active as a phonon trap, bottlenecking occurs because of resonant trapping of the phonons rather than boundary scattering. To estimate the excited-state concentration at which phonon bottlenecking comes in, we calculate the mean free path of the phonons against absorption by a Cr^{3+} ion in the lower Zeeman state of \bar{E} , and compare the result to the dimensions of the illuminated region. At a magnetic field of 50 kG at 45° to the c axis, corresponding to a Zeeman splitting of 4 cm^{-1} , we expect, according to Blume *et al.*,⁸ a direct relaxation time $T_{1d} \approx 50 \mu\text{s}$. The spectral width of the phonons on speaking terms can be estimated from the width of the excited-state EPR, observed by Geschwind *et al.*¹ to be $\Delta\nu \approx 60 \text{ MHz}$. Assuming coupling predominantly to the transverse branches, putting the sound velocity at $v = 6 \times 10^5 \text{ cm/s}$, and taking the density of phonon modes to be $\rho = 2 \times 10^6/\text{Hz cm}^3$, we estimate a mean free path $\Lambda = v\rho\Delta\nu T_{1d}/N^* \sim 400 \mu\text{m}$ for an excited-state concentration as low as $N^* \sim 10^{17}/\text{cm}^3$. Therefore, the direct relaxation process is anticipated to be heavily slowed down by phonon bottlenecking at the highest pumping, at which we may easily attain $N^* = 10^{18}/\text{cm}^3$ in a 700-ppm sample. Bottlenecking, of course, goes with Λ^{-1} , or through ρ and T_{1d} with $\sim H^3 \cos\theta \sin^2\theta$.

Summarizing this section, relaxation within the \bar{E} state is dominated by direct spin-lattice relaxation according to Eq. (1), provided the temperature is sufficiently low to suppress the Orbach relaxation via $2\bar{A}$. The relaxation must, however, be sufficiently fast not to be masked by $\tau_R \sim 4 \text{ ms}$, which requires fields of over, say, 30 kG at $\theta \sim 40^\circ$. Further, the excited-state concentration has to be reduced as much as possible to minimize bottleneck, while pulsed optical pumping is advantageous to eliminate spurious relaxation induced by bottlenecked 29 cm^{-1} phonons.

III. DISCUSSION OF EXPERIMENTS

We first present the experimental results on the field and angular dependence of the spontaneous direct relaxation of the upper Zeeman level of \bar{E} . Subsequently, we will consider both pulsed and continuous experiments at high pump levels to demonstrate strong imprisonment of resonant phonons generated in the nonradiative decay $\bar{E}_- \rightarrow \bar{E}_+$ of the optical pumping cycle.

The experimental arrangement consists of a 3 W

argon laser as a pumping source, the outgoing beam of which could be modulated by means of an acousto-optical crystal with a suppression of ~ 3000 and a risetime of $\sim 200 \text{ ns}$. The ruby crystal, containing 700-ppm Cr, is immersed in pumped liquid He held at a temperature of 1.5 K. Magnetic fields up to 65 kG are generated in a superconducting split-coil system. A double monochromator selects a particular component of the R_1 fluorescence emanating at right angles to the laser beam from the ruby crystal. A photomultiplier followed by conventional photon-counting electronics records the time development of the emitted light. A multichannel analyzer allowed time averaging of typically 50 000 passes through the decay, at a repetition rate several times slower than τ_R^{-1} .

A. Direct relaxation within \bar{E} in the limit of no bottleneck

1. Decay of fluorescence and temperature of the sample.

The ratio of the populations of the upper and lower Zeeman levels of \bar{E} (\bar{E}_+ and \bar{E}_- , respectively) immediately following a light pulse short compared to the time constants involved, T_{1d} and τ_R , is equal to the ratio of optical feeding constants into \bar{E}_+ and \bar{E}_- , or $N_+/N_- = \phi_+/\phi_-$. The relative feeding rates into \bar{E} , ϕ_\pm , are known to be determined by the spin memory in the optical pumping cycle.¹⁵ In case of high magnetic fields and low temperatures the population of the 4A_2 ground state is essentially in the lowest level, and the ratio $\phi_+/\phi_- = 0.2$ according to recent work.¹⁶ Therefore, immediately after the pulse the fluorescence from \bar{E}_+ is already weaker than that from \bar{E}_- , but still substantially above Boltzmann distribution. It is nevertheless easily distinguishable since its time evolution contains the decay of the direct process, which under appropriate experimental conditions is faster than τ_R . A typical decay of the \bar{E}_+ fluorescence is shown in Fig. 1. Here, balancing the conflicting conditions of low excited-state concentrations to suppress bottlenecking and of high pumping to obtain a satisfactory signal to noise ratio, we applied light pulses of $\sim 90 \mu\text{s}$ at maximum laser power, corresponding to exciting roughly 0.1% of the Cr^{3+} ions. Apart from the direct decay, an additional slower component shows up. The latter clearly does not find its origin in the background of the strong neighboring lines emanating from \bar{E}_- , but rather represents the radiative decay of the total \bar{E} population after \bar{E}_+ and \bar{E}_- have reached Boltzmann equilibrium via the direct process. From simple rate equation considerations it follows that the \bar{E}_+ population decays according to¹⁷

$$N_+ = a \exp[-t(1/T_{1d} + 1/\tau_R)] + b \exp(-t/\tau_R) \quad (2)$$

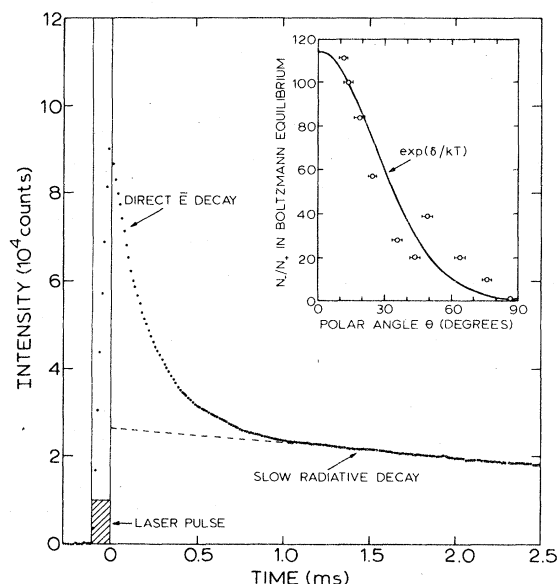


FIG. 1. Decay of the upper Zeeman level of the \bar{E} state in 700-ppm ruby at 1.5 K. The magnetic field is 43.3 kG at 64.5° to the c axis. The fast decay is due to the direct process within \bar{E} , while the slow one is the radiative decay of the total \bar{E} system in internal Boltzmann equilibrium. The inset shows the equilibrium population ratio within \bar{E} , deduced from extrapolating the slow part of the observed decay to $t=0$, vs the angle between a magnetic field of 43.3 kG and the c axis. The full curve represents the corresponding inverse Boltzmann factor for 1.5 K.

The ratio a/b is related to the relative optical feeding rates into \bar{E} and the inverse Boltzmann factor corresponding to the Zeeman splitting δ of \bar{E} through

$$\frac{a}{b} = \frac{\phi_+}{\phi_+ + \phi_-} (e^{\delta/kT} + 1) - 1 \quad (3)$$

For the data in a magnetic field of 43.3 kG, the inverse Boltzmann factors $\exp(\delta/kT)$ obtained from Eq. (3) are plotted in the inset of Fig. 1 as a function of the angle θ of the field to the c axis. Here, corrections have been applied for direct decay within \bar{E} taking place during the $90\text{-}\mu\text{s}$ pumping period. An interesting point is that these results allow the *in situ* determination of the temperature of the specimen just following excitation by adjusting the temperature in the Boltzmann factor. The full curve in the inset of Fig. 1 represents $\exp(\delta/kT)$ as a function of θ for $T = 1.5$ K, with δ calculated with $g_{\parallel} = 2.445$,¹ and $g_{\perp} \approx 0$.¹⁸ In the following we will adopt the fitted value of 1.5 K as the internal temperature of the crystal.

2. Magnetic field dependence and angular dependence of the direct process.

The results for the direct relaxation rate within \bar{E} at 1.5 K versus magnetic field at a polar angle of 11.5°

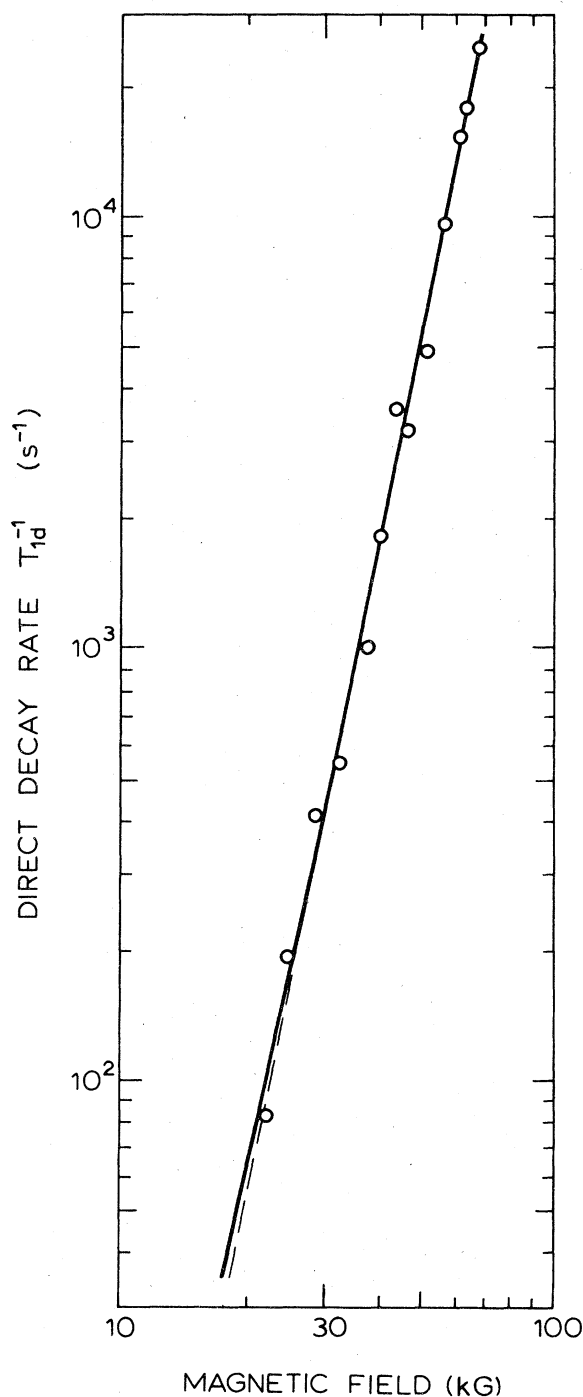


FIG. 2. Direct relaxation rate within the \bar{E} state at 1.5 K vs magnetic field at 11.5° to the c axis. The rates have been corrected for radiative decay and residual bottlenecking. The full curve represents Eq. (1), i.e., a fifth-power dependence on field, apart from a minor correction below 20 kG, due to the finite temperature, for the $\coth(\delta/2kT)$ appearing in Eq. (1).

are presented in Fig. 2. Again, 90- μ s excitation was used. A small angle was chosen to further reduce the bottlenecking correction, which scales with $\cos\theta\sin^2\theta$ for a Debye density of phonon modes and a constant phonon lifetime. Despite the reduction of pumping light and polar angle, some correction appeared to be necessary to eliminate residual slowing down by bottlenecking, amounting to up to 5% at the highest fields. Details on this correction are deferred to the more pertinent Sec. III B. In the analysis of the decays, the fast part, i.e., the a component in Eq. (2), was corrected for τ_R to extract the T_{1d} 's in Fig. 2. At a field of 14 kG a decay time of 4.35 ms was observed, which may be identified to τ_R of the \bar{E}_+ level, since at such a low field the direct decay is slower by two orders of magnitude. At 1.5 K, however, τ_R gradually decreases with increasing field to its untrapped value of 3.7 ms,¹ since the terminal level of the decay to 4A_2 becomes depopulated. In this connection, it is further noted that the effect of τ_R parallel to T_{1d} quickly loses importance with field. The results on the variation of the relaxation rate of the \bar{E}_+ level with the angle of the magnetic field are collected in Fig. 3 for 43.3 kG and 1.5 K. Again, the measurements have been corrected for the presence of weak bottlenecking (bottlenecking factors σ up to 0.4 around $\theta=60^\circ$), which, because of the nonexponential character of the decay due to temporal variation of σ , is the main source of the vertical error bars in Fig. 3. Since the splitting of the 4A_2 ground state, and thus its population distribution, does not substantially change with angle, the minor correction due to radiative decay to be subtracted from the observed rates has been taken independent of θ ($\tau_R=3.9$ ms). The error in θ is estimated to be 1.5° .

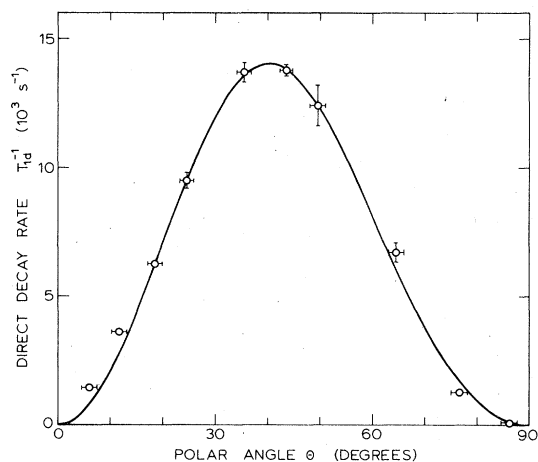


FIG. 3. Angular dependence of the direct relaxation within \bar{E} , corrected for radiative decay and residual bottlenecking at 43.3 kG and 1.5 K. The full curve, a fit of Eq. (1) to the data, is according to $\cos^3\theta\sin^2\theta\coth(\delta/2kT)$.

We now compare the data on the relaxation within \bar{E} to the behavior of the direct process predicted by Blume *et al.* The full drawn curves in Figs. 2 and 3 are fits of Eq. (1) to the data for 1.5 K, yielding a proportionality factor of $4.7 \times 10^{-19} \text{ G}^{-5} \text{ s}^{-1}$, within a factor of two equal to the value calculated in Ref. 8. It should be emphasized that, in contrast to previous experiments on direct relaxation, we are in a regime where $\delta > kT$, i.e., the thermal phonon occupations are much smaller than unity and the decays are virtually spontaneous. In Fig. 2, $\coth(\delta/2kT)$ deviates from unity by less than 3% above say 35 kG, so that T_{1d}^{-1} essentially varies with the fifth power of the field; in the low-field region there is a slight deviation from H^5 , increasing to 18% at 22 kG. In Fig. 3, temperature plays a role only at the larger θ , amounting to $\coth(\delta/2kT)=1.4$ at 70° . In view of the excellent accord between experiments and Eq. (1) with respect to the functional dependences on H and θ , while, in addition, the prefactor agrees within the uncertainties of the parameters involved, the results of Figs. 2 and 3 unambiguously demonstrate that the direct process considered by Blume *et al.* indeed is the dominant decay process within \bar{E} . We note, however, that Eq. (1) appears to slightly underestimate the data at low angles ($\theta < 15^\circ$) in Fig. 3. We suggest that this speedup of the observed rate is indicative of a direct process originating from configurational mixing as treated by Kiel,¹³ which is operative in a magnetic field *parallel* to the c axis. Taking into account the correction to the Kiel formulas suggested in Ref. 8, we find a rough estimate of $\sim 250 \text{ s}^{-1}$ for the direct rate at 43.3 kG along the c axis, which is of the right order of magnitude to explain the deviation.

B. Bottlenecking of the direct process

As discussed in Sec. II, bottlenecking of phonons generated in the optical pumping cycle in the transition $\bar{E}_+ \rightarrow \bar{E}_-$ is anticipated at high concentrations of Cr^{3+} ions in the excited \bar{E}_- state. In this part, we will consider measurements on the relaxation within the Kramers doublet \bar{E} at high optical pump levels. Pulsed experiments will reveal a slowing down of the direct relaxation by over an order of magnitude upon increasing N_- , demonstrating unambiguously the bottlenecking of the energy transport to the bath by the phonons on speaking terms with the transition. The analysis of the data is based on rate equations governing ion and phonon occupations. In passing, the corrections on the data points presented in Figs. 2 and 3 will be clarified. Finally, in steady-state experiments at high excitation the population of the \bar{E}_+ level is observed to increase by at least an order of magnitude above Boltzmann equilibrium.

1. Direct decay rate under bottlenecking conditions.

In Fig. 4, measurements at 1.5 K on the direct relaxation rate as a function of the excited-state con-

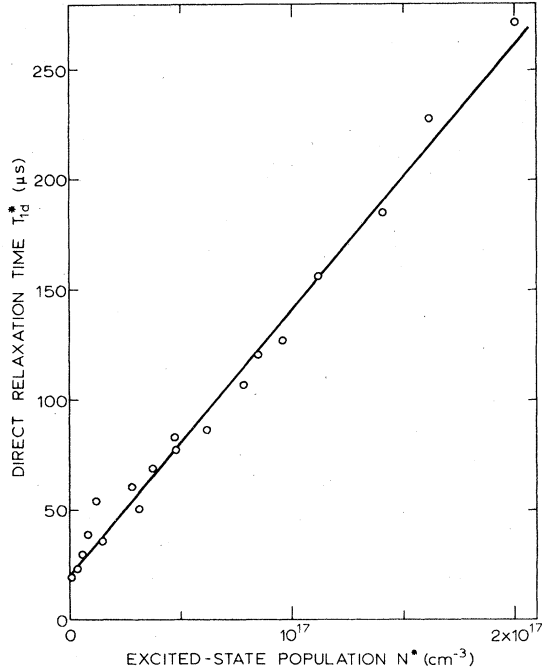


FIG. 4. Direct relaxation time of the \bar{E}_+ level vs excited state population N^* in a magnetic field of 56.5 kG at $\theta = 40^\circ$ to the c axis. The slowing down up to a factor of $1 + \sigma = 14$ is due to multiple interruptions of the resonant phonons. N^* is estimated from the bottlenecked ratio R_2/R_1 .

centration N^* are presented. The acousto-optical modulator is adjusted to a pulse length of 3.2 ms, in order to integrate N^* over a time interval of the order of the radiative lifetime prior to observation of the decays. The intensity is varied by inserting calibrated neutral density filters into the pulsed beam. In order to couple the phonons to the Cr^{3+} ions in the \bar{E} state as strongly as allowed by the apparatus, the field was set to 56.5 kG, close to quenching of the superconducting magnet at high optical pumping, at an angle of 40° . Under these conditions, N_+ appeared to be less than 1% of N_- , due to the small Boltzmann factor ($\delta/kT \approx 5$), and therefore all of the population of the metastable states of 2E is in \bar{E}_- , or $N^* \approx N_-$. A linear increase of the bottlenecked direct relaxation time T_{1d} , up to a factor of ~ 14 , is found with increasing N^* .

In order to estimate the phonon lifetime we set up a simple description of the phonon bottleneck in the spirit of Brya *et al.*,¹¹ and apply this to the ruby case. The situation differs, however, from EPR ground-state experiments in that $N_- \gg N_+$, rather than $N_- \approx N_+$. The rate equations describing the time development of the populations of the two Kramer states \bar{E}_+ and \bar{E}_- can be written, after switching off

the optical pumping, as

$$\frac{dN_-}{dt} = \frac{(1+p)N_+}{T_{1d}^{(s)}} - \frac{pN_-}{T_{1d}^{(s)}} - \frac{N_-}{\tau_{R-}}, \quad (4a)$$

$$\frac{dN_+}{dt} = -\frac{(1+p)N_+}{T_{1d}^{(s)}} + \frac{pN_-}{T_{1d}^{(s)}} - \frac{N_+}{\tau_{R+}}, \quad (4b)$$

where $T_{1d}^{(s)-1} \propto H^5 \cos^3 \theta \sin^2 \theta$ is the spontaneous direct relaxation rate from \bar{E}_+ to \bar{E}_- , τ_{R+} and τ_{R-} are the radiative lifetimes of the Zeeman levels of \bar{E} , which are not necessarily equal to each other due to reabsorption of the fluorescence, and p is the occupation number of the phonons on speaking terms with the transition; $N_+ + N_- = N^*$. The multiple interruption of these phonons due to the trapping by the Cr^{3+} ions can be formulated in the form of the rate equation

$$\frac{\rho \Delta \nu dp}{dt} = \frac{(1+p)N_+}{T_{1d}^{(s)}} - \frac{pN_-}{T_{1d}^{(s)}} - \frac{\rho \Delta \nu (p - p_0)}{\tau}, \quad (5)$$

in which we assume, for simplicity, a square phonon packet of width $\Delta \nu$; ρ is the density of phonon modes per frequency interval at the resonance frequency, p_0 is the thermal phonon occupation number, and τ is the phonon lifetime. In general these equations have no analytical solution. However, since we are only interested in the decay on the time scale T_{1d} , the phonon system, which adjusts itself on the much faster time scale τ , may be considered in equilibrium, i.e., $dp/dt = 0$. Then, we have from Eq. (5)

$$p = \frac{N_+/T_{1d}^{(s)} + \rho \Delta \nu p_0/\tau}{\Delta N/T_{1d}^{(s)} + \rho \Delta \nu/\tau}, \quad (6)$$

with $\Delta N = N_- - N_+$. Substituting this into Eq. (4), we have

$$\frac{dN_+}{dt} = -\left[\frac{1+2p_0}{(1+\sigma)T_{1d}^{(s)}} + \frac{1}{\tau_{R+}} \right] N_+ + \frac{p_0 N^*}{(1+\sigma)T_{1d}^{(s)}}, \quad (7)$$

where we have introduced the bottlenecking parameter

$$\sigma = \tau \Delta N / \rho \Delta \nu T_{1d}^{(s)}. \quad (8)$$

According to Ref. 19, the time interval $\rho \Delta \nu T_{1d}^{(s)} / \Delta N$ is equal to the average time a phonon spends between the emission and the reabsorption by Cr^{3+} ions in the excited \bar{E} state. Therefore, σ represents the number of interruptions the phonon suffers within its lifetime τ . Of course, σ will vary with ΔN during the decay under bottlenecking conditions. In the present experiments, however, $N_- \gg N_+$, or $\Delta N \approx N^*$, so that on the time scale $T_{1d} \ll \tau_R$, σ is essentially constant, and the decay is unieponential with a characteristic time

$$T_{1d}^* = T_{1d}(1 + \sigma), \quad (9)$$

in parallel to τ_R .

Returning to Fig. 4, we see that Eq. (9) indeed represents the observed linear increase of the data up to an observed $\sigma \approx 13$. Fitting Eq. (9) to the data, we find $T_{1d} = 20 \pm 2 \mu\text{s}$, which, because $\coth(\delta/2kT) = 1$, essentially equals the spontaneous decay time $T_1^{(g)}$ at $H = 56.5 \text{ kG}$ and $\theta = 40^\circ$. We now can estimate τ by substituting the relevant parameters in Eq. (8). Assuming the coupling to the transverse mode dominant, we take the number of phonon modes on speaking terms equal to the transverse $\rho\Delta\nu = 2 \times 10^{14}/\text{cm}^3$, with the spectral width of the phonons equal to the half-width of the EPR measured by Geschwind *et al.*¹ The metastable population density N^* can be estimated from the observed ratio of the fluorescent R_2 and R_1 intensities upon stationary pumping by use of Fig. 1 in a previous paper,³ yielding a maximum $N^* \sim 2 \times 10^{17}/\text{cm}^3$ in Fig. 4. The maximum value of σ reached in the experiments of Fig. 4 is 13, and substituting the above estimates in Eq. (8), we finally obtain a phonon lifetime $\tau \sim 0.2 \mu\text{s}$. A lifetime of $0.2 \mu\text{s}$ for the 5 cm^{-1} phonons resonant within \bar{E} cannot originate from anharmonic decay, as has been proposed for 29 cm^{-1} phonons in ruby,^{2,4} since at low temperatures the anharmonic lifetime scales with $1/\nu^5$,²⁰ and would be of the order of milliseconds. Instead, in view of the fact that the path travelled by the phonons in $0.2 \mu\text{s}$ (about 1 mm) is of the order of the characteristic dimension L of the illuminated region (a cylinder with diameter of about 0.3 mm and length of 4 mm), we suggest τ to originate from ballistic phonon transport to the edge of the excited region. In this context, we note that by putting $\tau = L/\nu$ in Eq. (8), Eq. (9) becomes identical to the result of Giordmaine *et al.*¹⁹ for *marginal* trapping [See Eq. (5) in their paper].

Although Eq. (9) represents the behavior of the data (Fig. 4), there remains a problem of conceptual nature. In the present experiments σ reaches values of about 13, so that the condition of marginal trapping is not fulfilled. Since for $\sigma \gg 1$ the mean free path of the phonons is shorter than L , a random walk of the phonons to the border of the illuminated region occurs in the absence of other phonon loss mechanisms,⁵ in which case a quadratic dependence on the excited-state concentration should have been observed [see Eq. (4') in Ref. 19]. This is not found in the experiments. If we consider a shape of the spectral line more realistic than a square packet, the phonons resonant in the wings of the line have a mean free path comparable to at least the dimensions of the excited region. If, in addition, fast spectral redistribution exists within the resonance line, the phonons in the core of the resonance line will have access to those in the more transparent wings, which in turn will transport the energy to the nonexcited region of the crystal. For the present case of an essentially Gaussian resonance line,¹ the result for T_{1d}^* in

case of severe trapping, Eq. (7') in Ref. 19, is identical to our Eq. (9), apart from a weakly varying logarithmic factor. The conclusion is that bottlenecking of the direct process in 700-ppm ruby is accompanied by fast spectral redistribution operative within the resonance line. As to the mechanisms for spectral redistribution, in a two-level system any change in phonon frequency must occur when the system is in the upper level during the imprisonment time T_{1d} of the phonon. As the main origin of the broadening of the Cr^{3+} EPR in \bar{E} seems to be inhomogeneous superhyperfine interaction with the surrounding Al nuclear spins,²¹ spin-spin relaxation of the Al nuclei, which is fast relative to T_{1d} ,²² is the most likely source for redistribution. Additional redistribution could be provided by dipolar broadening among the excited Cr^{3+} and those in the 4A_2 state.

Finally, we return to the corrections for bottlenecking to arrive at Figs. 2 and 3 presented in Sec. III A. The weak-bottleneck data were obtained at essentially the same N^* . They were tied to Fig. 4 by use of Eqs. (1) and (9), where σ was adopted to be proportional to $H^3 \cos\theta \sin^2\theta$, in accordance with a Debye density of modes and a frequency-independent phonon lifetime. The resulting σ for $H = 56.5 \text{ kG}$ and $\theta = 40^\circ$ (≈ 0.4) was subsequently rescaled to the particular H and θ to correct the measured times to the unbottlenecked ones.

2. Ratio N_+/N_- under steady-state bottlenecking conditions.

In view of the prolonging of the direct relaxation time within \bar{E} already at excited-state populations of the order of $\sim 10^{17}/\text{cm}^3$ due to bottlenecking of the phonons generated in the decay $\bar{E}_+ \rightarrow \bar{E}_-$, it is anticipated that under the conditions of severe *continuous* pumping the ratio N_+/N_- , or the fraction N_+/N^* , will deviate from its low-pump value. The situation is very similar to the $2\bar{A} \rightarrow \bar{E}$ transition, where bottlenecking of optically generated 29 cm^{-1} phonons has been found to dramatically affect the R_2/R_1 fluorescent intensity ratio.^{3,5} The fraction N_+/N^* under continuous optical pumping with a focussed laser beam is presented in Fig. 5 as a function of the total excited-state population N^* , otherwise under the conditions of Fig. 4, i.e., a temperature of 1.5 K and a magnetic field of 56.5 kG at 40° to the c axis ($\delta = 5.3 \text{ cm}^{-1}$). Again, the intensity of the pumping light is varied by means of a set of neutral density filters. At low concentrations, a constant N_+/N^* is found, while upon raising N^* an increase of the fraction by an order of magnitude is observed. Because of the different matrix elements and reabsorptions of the various R_1 Zeeman components, the data are normalized to the nonbottlenecked ratio.

In order to demonstrate the consistency of these measurements with the time-resolved experiments of

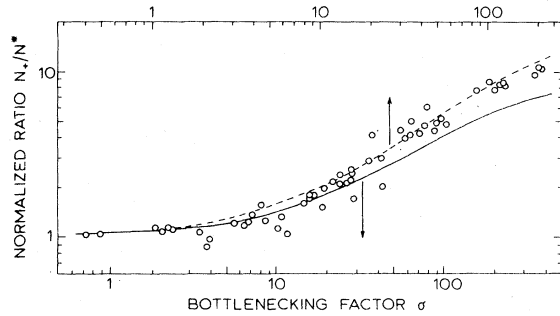


FIG. 5. Fractional population N_+/N^* of \bar{E}_+ , normalized to absence of bottleneck, vs the bottlenecking factor σ , adjusted according to Eq. (10). The full curve corresponds to $\phi_+/\phi_- = 0.2$, yielding $N_+/N^* = 0.01$ at very low σ ; the dashed curve accounts for redistribution of the feeding by 29 cm^{-1} phonons, as expressed in an effective $\phi_+/\phi_- = 0.7$.

Fig. 4, we apply Eq. (7) to the case of stationary optical pumping. Accordingly, we set the optical feeding rate into the \bar{E}_+ level, $\phi_+ N^*$, equal to the time derivative of N_+ and solve the resultant equation, yielding for the fractional population of the upper Zeeman component of \bar{E}

$$\frac{N_+}{N^*} = \frac{p_0 + \phi_+ T_1^{(s)}(1 + \sigma)}{1 + 2p_0 + T_1^{(s)}(1 + \sigma)/\tau_{R+}} \quad (10)$$

Note that $N_+/N^* \approx N_+/N_-$. At low excited-state populations ($\sigma < 1$), N_+/N^* has a constant value of $(p_0 + \phi_+ T_1^{(s)})/(1 + 2p_0 T_1^{(s)}/\tau_{R+})$, determined by thermal background and optical feeding, but at 1.5 K primarily by the former. Towards higher values of σ , N_+/N^* increases, until at the highest bottlenecking a new constant level equal to $\phi_+ \tau_{R+}$ is reached, corresponding to the situation of a bottlenecked direct decay within \bar{E} that can no longer compete with the radiative decay.

To compare Eq. (10) to the data points of Fig. 5, we first substitute the Bose factor $p_0 = 1.0 \times 10^{-2}$ at 1.5 K, given δ . For the ratio of the feeding constants we adopt $\phi_+/\phi_- = 0.2$ according to Ref. 16, which, noting that R_1 mainly departs from \bar{E}_- , corresponds to $\phi_+ = 0.2/1.2\tau_{R-}$, or with $\tau_{R-} = 6.7 \text{ ms}$, $\phi_+ = 25 \text{ s}^{-1}$. Finally, $T_1^{(s)} \approx 20 \mu\text{s}$ under the present conditions. From Eq. (10) we thus obtain N_+/N^* vs σ , where according to Eq. (8) σ is proportional to N^* . The result is represented in Fig. 5 by the full line, after horizontal adjustment to the low-bottleneck regime ($\delta < 20$). The horizontal calibration thus obtained has, of course, to comply with rough estimates for N^* from R_2/R_1 as well as R_1 . We then estimate a maximum attainable $N^* \sim 5 \times 10^{18}/\text{cm}^3$ in 700 ppm, corresponding to $\sigma \sim 300$, larger than in the time-resolved experiments mainly because the acousto-optical modulator could be left out. In comparing the full curve to the data, we see that the variation of

N_+/N^* with pump intensity is indeed generally consistent with the idea of bottlenecking of optically generated 5 cm^{-1} phonons, despite the fact that at bottlenecking substantially beyond that in Fig. 4 ($\sigma > 50$) the increase of N_+/N^* is clearly underestimated.

Two explanations for the deviation at high σ are considered here. First, we note that a good fit to the shape of the data would have been obtained for a Bose factor of 2×10^{-3} , corresponding to a sample temperature of 1.2 K. However, a sample temperature around 1.5 K is more realistic. Secondly, in the continuous case we have to consider the effects of Orbach-type processes connecting the two Kramers levels of \bar{E} via the $2\bar{A}$ state 29 cm^{-1} above. In effect, as discussed in Sec. II, these optically induced Orbach processes redistribute the optical feeding into the $2\bar{A}$ level over the two Zeeman levels of \bar{E} , i.e., the ratio ϕ_+/ϕ_- is changed as compared to the non-bottlenecked value of Ref. 16. The following qualitative experiment was carried out to support this. The populations of $2\bar{A}_{\pm}$ were monitored through the R_2 Zeeman lines as a function of a magnetic field at 40° to the c axis. It is found that, starting from zero field, the R_2 intensities drop by orders of magnitude, until at 56 kG the lines are hardly discernable. We note that at low fields the direct \bar{E} relaxation is masked by radiative decay, and therefore $N_+ \sim N_-$. Accordingly, the phonons on speaking terms with the transitions $\bar{E}_+ \leftrightarrow 2\bar{A}_{\pm}$ are about equally trapped as those resonant with $\bar{E}_- \leftrightarrow 2\bar{A}_{\pm}$. In contrast, at 56 kG N_+ is smaller than N_- by at least an order of magnitude, and the phonons associated with \bar{E}_+ experience the lattice as more transparent. As a result the part of the optical feeding of \bar{E} via $2\bar{A}$, being $1/2.6$ of the direct feeding into \bar{E} ,¹⁴ will eventually terminate in \bar{E}_+ . If we assume the ratio of the direct feeding constants into \bar{E} due to the spin memory alone to be 0.2, we have for the present situation an effective ϕ_+/ϕ_- of 0.7, yielding $\phi_+ \approx 60 \text{ s}^{-1}$. Adopting this value for ϕ_+ , Eq. (9) at 1.5 K results in the dashed curve in Fig. 5, i.e., the dashed curve corresponds to a maximum two-phonon redistribution within 2E . A good fit to the data is obtained, demonstrating consistency between the time-resolved and continuous experiments.

IV. CONCLUSIONS

The direct relaxation within the \bar{E} state of ruby has been investigated. Excellent agreement has been found between the experimental results at low-optical pump levels and theoretical predictions by Blume *et al.*, with special emphasis on the fifth-power dependence on the magnetic field and the $\cos^3\theta \sin^2\theta$ dependence on the orientation. Also the prefactor calculated by Blume *et al.* from static data turned out to be near experiment. Thus, the ruby system pro-

vided an exceptionally sensitive verification of direct spin-lattice relaxation theory.

Secondly, quite similar to earlier experiments on 29 cm^{-1} phonons resonant between \bar{E} and $2\bar{A}$, bottlenecking of the direct process produced by increasing the optical pumping was detected both in pulsed experiments through the slowing down of the direct decay, and in stationary experiments by monitoring the nonlinear increase of the \bar{E}_+ population. A consistent description for these observations could be arrived at assuming a constant phonon lifetime of the order of the transit time through the illuminated region. To explain such a linear phonon-loss mechanism up to the observed bottlenecking factors of ~ 200 , fast spectral redistribution is suggested to take place, producing spectral contact between the phonons in the core of the resonance line and those in the wings. Due to the nonresonant character, these experiments on phonon trapping may easily be extended to a wider range of resonance frequencies as well as variation of the opacity and the dimensions of the trapping region.

We finally consider the capabilities that the direct process within \bar{E} has in acting as a tunable narrow bandwidth phonon detector and generator. Acting as a detector, the system should have a high concentration of Cr^{3+} in \bar{E}_- , as under severe pumping, making

it opaque to phonons fitting $\bar{E}_- \rightarrow \bar{E}_+$. Particular advantages of the detector are its bandwidth, which, essentially equal to that of the transition ($\approx 0.002 \text{ cm}^{-1}$), is extremely narrow compared to other level schemes suited for phonon detection, and its sensitivity through optical detection. The absorptive rate, scaling with $T_{1d}^{(s)-1}$, would be highest near $\theta = 40^\circ$. Tuning would simply require varying the field. The highest frequencies are in practice set by the limitation of laboratory magnets, say 12 T, corresponding to 15 cm^{-1} ; the lower limit has to do with the efficiency, which severely drops when T_{1d} becomes comparable to τ_R , say at 2 cm^{-1} . Another limiting factor for a detector is the mean free path, which however at $N^* = 10^{19}/\text{cm}^3$, easily attainable in a slightly more concentrated ruby than we used, is less than 1 mm at a splitting smaller than 1 cm^{-1} . Phonon generation by the \bar{E} system is simply accomplished by the nonradiative decay $\bar{E}_+ \rightarrow \bar{E}_-$. The characteristics, regarding the bandwidth and the tuning range, are of course similar to those of the detector. Angles somewhat smaller than $\theta \approx 40^\circ$ are probably more favorable here to reduce resonant absorption. A final point to note is that inversion of the \bar{E} populations with dye-laser excitation of \bar{E}_+ would, under appropriate conditions, open new perspectives for phonon amplification and spin-phonon super-radiance.

- ¹S. Geschwind, G. E. Devlin, R. L. Cohen, and S. R. Chinn, *Phys. Rev.* **137**, A1087 (1965).
- ²K. F. Renk and J. Deisenhofer, *Phys. Rev. Lett.* **26**, 764 (1971); K. F. Renk and J. Peckenzell, *J. Phys. (Paris)* **33**, C4-103 (1972).
- ³J. I. Dijkhuis, A. van der Pol, and H. W. de Wijn, *Phys. Rev. Lett.* **37**, 1554 (1976).
- ⁴R. S. Meltzer and J. E. Rives, *Phys. Rev. Lett.* **38**, 421 (1977).
- ⁵J. I. Dijkhuis and H. W. de Wijn, *Phys. Rev. B* **20**, 1844 (1979) (following paper).
- ⁶T. Holstein, S. K. Lyo, and R. Orbach, *Phys. Rev. Lett.* **36**, 891 (1976); *Phys. Rev. B* **15**, 4693 (1977).
- ⁷J. Koo, L. R. Walker, and S. Geschwind, *Phys. Rev. Lett.* **35**, 1669 (1975).
- ⁸M. Blume, R. Orbach, A. Kiel, and S. Geschwind, *Phys. Rev.* **139**, A314 (1965).
- ⁹See *Spin-Lattice Relaxation in Solids*, edited by A. A. Manenkov and R. Orbach (Harper and Row, New York, 1966).
- ¹⁰Amar Singh and R. C. Sapp, *Phys. Rev. B* **5**, 1688 (1973).
- ¹¹W. J. Brya and P. E. Wagner, *Phys. Rev.* **147**, 239 (1966).
- ¹²J. M. Baker and N. C. Ford, *Phys. Rev.* **136**, A1692 (1964).
- ¹³A. Kiel, in *Advances in Quantum Electronics*, edited by J. R. Singer (Columbia University, New York, 1961), p. 417.
- ¹⁴J. E. Rives and R. S. Meltzer, *Phys. Rev. B* **16**, 1808 (1977).
- ¹⁵G. F. Imbusch and S. Geschwind, *Phys. Rev. Lett.* **17**, 238 (1966).
- ¹⁶H. W. de Wijn and R. Adde, *Solid State Commun.* **27**, 1285 (1978).
- ¹⁷Unbalance of the radiative decay times of \bar{E}_+ and \bar{E}_- due to reabsorption can easily be incorporated, without essentially modifying the results for T_{1d} .
- ¹⁸T. Muramoto, *J. Phys. Soc. Jpn.* **35**, 921 (1973).
- ¹⁹J. A. Giordmaine and F. R. Nash, *Phys. Rev.* **138**, A1510 (1965).
- ²⁰P. G. Klemens, *J. Appl. Phys.* **38**, 4573 (1967).
- ²¹W. J. C. Grant and M. P. W. Strandberg, *Phys. Rev.* **135**, A727 (1964); R. F. Wenzel, *Phys. Rev. B* **1**, 3109 (1970); R. Boscaino, M. Brai, and I. Ciccarello, *Phys. Rev. B* **13**, 2798 (1976).
- ²²C. M. Verber, H. P. Mahon, and W. H. Tantilla, *Phys. Rev.* **125**, 1149 (1962).